Cellular/Molecular

NMDA Receptors Increase the Size of GABAergic Terminals and Enhance GABA Release

Mónica L. Fiszman,[1,2] Andrea Barberis,[1] Congyi Lu,[1] Zhanyan Fu,[1] Ferenc Erdélyi,[3] Gábor Szabó,[3] and Stefano Vicini[1]

[1]Department of Physiology and Biophysics, Georgetown University School of Medicine, Washington, DC 20007, [2]Instituto de Investigaciones Farmacológicas, Consejo Nacional de Investigaciones Científicas y Técnicas, 1113 Buenos Aires, Argentina, and [3]Laboratory of Molecular Biology and Genetics, Institute of Experimental Medicine, H-1450 Budapest, Hungary

In developing cerebellar interneurons, NMDA increases spontaneous GABA release by activating presynaptic NMDA receptors. We investigated the role of these receptors on differentiating basket/stellate cells in cerebellar cultures grown under conditions allowing functional synaptic transmission. Presynaptic GABAergic boutons were visualized either by GAD65 immunostaining or by using cells derived from GAD65– enhanced green fluorescent protein (eGFP) transgenic mice, in which cerebellar basket/stellate cells express eGFP. After the first week in culture, whole-cell recordings from granule cells reveal that acute application of NMDA increases miniature IPSC (mIPSC) frequency. Interestingly, after 2 weeks, the mIPSC frequency increases compared with the first week but is not modulated by NMDA. Furthermore, in cultures chronically treated with NMDA for 1 week, the size of the GABAergic boutons increases. This growth is paralleled by increased mIPSC frequency and the loss of NMDA sensitivity. Direct patch-clamp recording from these presynaptic terminals reveals single NMDA-activated channels, showing multiple conductance levels, and electronic propagation from the somatodendritic compartment. Our results demonstrate that NMDA receptors alter GABAergic synapses in developing cerebellar cultures by increasing the size of the terminal and spontaneous GABA release. These findings parallel changes in inhibitory synaptic efficacy seen *in vivo* in developing GABAergic interneurons of the molecular layer of the cerebellum.

Key words: **cerebellum; synapses; interneuron; patch clamp; GFP; BDNF**

Introduction

Activity in the brain is sculpted by the interplay between excitatory and inhibitory synapses. A fundamental link between excitation and inhibition lays in the role of ionotropic glutamate receptors on both the differentiation of GABAergic interneurons and release from their presynaptic terminals. Increased motility of axonal filopodia induced by presynaptic or axonal AMPA and kainate receptors has been reported previously (Chang and De Camilli, 2001; Tashiro et al., 2003). Furthermore, an increase in the number of presynaptic releasable pools by cAMP requires NMDA and non-NMDA receptor activation (Ma et al., 1999). Cerebellar basket/stellate interneurons are early examples in which interplay of excitation and inhibition has been reported. These neurons reach the molecular layer postnatally, where they are innervated by granule cell axons (parallel fibers) that provide glutamatergic inputs (Eccles et al., 1967; Palay and Chan-Palay, 1974). Synaptic efficacy of these cerebellar interneurons changes with development (Pouzat and Hestrin, 1997; Bureau and Mulle, 1998), and activation of ionotropic glutamate receptors increases the occurrence of miniature IPSCs (mIPSCs) (Bureau and Mulle, 1998; Glitsch and Marty, 1999; Duguid and Smart, 2004; Huang and Bordey, 2004). Indirect evidence from these studies suggested that NMDA receptors are localized on GABAergic axons. This is supported by anatomical evidence that NMDA receptor subunit immunostaining is found on molecular layer interneurons in culture (Duguid and Smart, 2004) and on axonal "pinceau" of basket cells (Petralia et al., 1994). It has been demonstrated recently that the increase in NMDA-induced mIPSC frequency is regulated by glial glutamate transporters (Huang and Bordey, 2004) and has a physiological role in a newly identified form of inhibitory synaptic plasticity (Duguid and Smart, 2004).

The availability of transgenic mice that express enhanced green fluorescent protein (eGFP) driven by the GAD65 promoter (Brager et al., 2003; Galarreta et al., 2004; Lopez-Benedito et al., 2004) allows direct visualization of GABAergic interneurons and the fine features of their axonal and synaptic processes. The development of functional inhibitory synapses can be studied in primary cultures of cerebellar cells (Virginio et al., 1995; Ueno et al., 1996; Mellor et al., 1998; Ortinski et al., 2004). This culture can be used as a model of cerebellar interneuronal development, which allows direct measurements of synaptic function. Molecular mechanisms involved in neuronal development have been widely investigated using this experimental system (Gallo et al., 1987; Resink et al., 1996; Borodinsky et al., 2002; Studler et al., 2002). To understand more about the mod-

Received July 2, 2004; revised Jan. 4, 2005; accepted Jan. 7, 2005.

This work was supported by National Institutes of Health Grants MH64797 and NS047700 to S.V. and National Office for Research and Technology Grant OBFB-00498/2002J to G.S. We thank Dr. Enrico Mugnaini (Northwestern University Medical School, Chicago, IL) for providing the GAD65– eGFP mice derived from Dr. Szabó's laboratory, Brian Robertson (University of Leeds, Leeds, UK) for critical reading of this manuscript, and Dr. Stephen M. Logan and Jose A. Matta (Georgetown University, Washington, DC) and Dr. Gabriele Losi (University of Modena, Modena, Italy) for participating in some experiments.

Correspondence should be addressed to Dr. Stefano Vicini, Department of Physiology and Biophysics, Basic Science Building 225, Georgetown University School of Medicine, 3900 Reservoir Road, Washington, DC 20007. E-mail: svicin01@georgetown.edu.

DOI:10.1523/JNEUROSCI.4980-04.2005

 0270-6474/05/252024-08$15.00/0

ulation of inhibitory synapses by NMDA, we investigated the development of GABAergic inhibitory synaptic transmission using primary cerebellar culture from GAD65–eGFP mice. We verified that the reported presynaptic action of NMDA on mIPSC frequency in cerebellar interneurons can be reproduced in primary culture. We then investigated the long-term effect of NMDA on functional and morphological correlates of inhibitory synaptic transmission in differentiating basket/stellate cells. Our results show that in cultures grown for 7 d, chronic exposure to NMDA increases the size of GABAergic boutons and the frequency of mIPSCs but reduced the potentiation of inhibition induced by acute exposure to NMDA. We conclude that there is a powerful control of NMDA receptors on GABAergic inhibitory neurotransmission in developing interneurons.

Materials and Methods

Cerebellar cell cultures, immunocytochemistry, and dye loading. Primary cultures of mouse cerebellum were prepared from postnatal day 6–8 mice. Mouse pups were killed by decapitation in agreement with the guidelines of the Georgetown University Animal Care and Use Committee. Cerebella were dissociated with trypsin (0.25 mg/ml; Sigma, St. Louis, MO) and plated in 35 mm Nunc (Roskilde, Denmark) dishes at a density of 1.1×10^6 cells/ml on glass coverslips (Fisher Scientific, Pittsburgh, PA) coated with poly-L-lysine (10 μg/ml; Sigma). The cells were cultured in basal Eagle's medium supplemented with 10% fetal bovine serum, 2 mM glutamine, 20 μg/ml gentamycin (all from Invitrogen Carlsbad, CA), 0.1 mg/ml transferrin, and 0.025 mg/ml insulin (Sigma). Cells were maintained at 37°C in 5% CO_2, and 10 μM cytosine arabinofuranoside (Sigma) was added at 3 d *in vitro* (DIV3). Culture treatments with NMDA, (+)-5-methyl-10,11-dihydro-5H-dibenzo [a,d] cycloheptene-5,10-imine maleate (MK801; Sigma), 50 ng/ml brain-derivedneurotrophic factor (BDNF), 10 μg/ml anti-BDNF antibody (Alomone Laboratories, Jerusalem, Israel), or 25 mM KCl were performed at DIV2 for various time periods as described. MK801 and anti-BDNF were added 1 hr before the addition of agonists.

Live cultured neurons were fixed by incubation with 4% paraformaldehyde, 4% sucrose in PBS for 10 min, and washed three times in PBS (for GAD65 and synapsin 1) and with 2 min of 4% paraformaldehyde followed by 10 min with methanol, for vesicle-associated membrane protein 2 (VAMP2) and vesicle glutamate transporter-1 (vGlut-1) and vGlut-2. Fixed neurons were permeabilized with 0.3% Triton X-100/PBS for 5 min (GAD65 and synapsin 1), washed several times with PBS, and incubated in 10% bovine serum albumin in PBS for 1 hr to block nonspecific staining. Cells were then incubated for 1 hr with one of the following primary antibodies: GAD65 monoclonal antibody (GAD6; 1:1000; Developmental Studies Hybridoma Bank, University of Iowa, Iowa City, IA), rabbit anti-synapsin1 antibody (1:1000; Chemicon, Temecula, CA), rabbit anit-VAMP2 antibody (1:1000; Alomone Laboratories), and mouse anti-vGlut-1 (0.5 μg/ml) and anti-vGlut-2 (1 μg/ml; Synaptic System, Goettingen, Germany). After washing with PBS, cells were incubated with indocarbocyanine (Cy3)-conjugated secondary antibodies (1:1000; Jackson ImmunoResearch, West Grove, PA). All immunostaining experiments were performed at room temperature. For confocal imaging of cerebellar slices of GAD65–eGFP mice, animals were transcardially perfused under deep pentobarbital anesthesia (100 mg/kg of body weight, i.p.) with 4% paraformaldehyde in 0.1 M sodium phosphate buffer, pH 7.2. After dissection, brains were postfixed overnight, and microslicer sections (100 μm) were mounted and visualized with a LSM 510 META (Carl Zeiss, Oberkochen, Germany) confocal microscope using 60× oil objective [numerical aperture (NA), 1.4].

N-(3-triethylammoniumpropyl)-4-(6-(4-(diethylamino)phenyl) hexatrienyl) pyridinium dibromide (FM4-64) labeling was performed according to a modification of the procedure described by Krueger et al. (2003). Briefly, cultured cerebellar cells were superfused with HEPES-buffered saline (HBS) containing the following (in mM): 124 NaCl, 3 KCl, 2 $CaCl_2$, 1 $MgCl_2$, 10 HEPES, and 5 D-glucose, adjusted to pH 7.3. Loading was accomplished by switching to 15 μM FM4-64 (Molecular Probes) in a solution containing (in mM) 90 KCl, 37 NaCl, 2 $CaCl_2$, 1 $MgCl_2$, 10 HEPES, and 5 D-glucose supplemented with 10 μM NBQX and 50 μM APV for 45 s, followed by a washout period of 8 min. Cells were imaged within 15 min after washout.

Image analyses. Neurons were imaged on a Nikon (Tokyo, Japan) E600 microscope equipped with a 60×, 1.0 NA objective. Nikon bandpass filter cubes were used for Cy3 or eGFP fluorescence. Digital images were acquired with a CFW-1310 (Scion Corporation, Frederick, MD), 10-bit (1024 gray scale intensity level) CCD digital camera, 1360 × 1024 pixel array. Images were analyzed with MetaMorph (Universal Imaging, Downingtown, PA) and pseudocolored for presentation with Adobe Photoshop CS (Adobe Systems, San Jose, CA). The number and size of eGFP-containing boutons or those expressing presynaptic markers were determined in thresholded and randomly selected 10 μm axonal segments. At least 30 segments were analyzed in each experimental group from six separate cultures unless otherwise stated. Statistical comparisons were done using a two-tailed Student's *t* test assuming homogeneity of variances of the samples with Bonferroni corrections. Data values are expressed as mean ± SEM.

Electrophysiology. Coverslips with cerebellar neurons were placed on the stage of an inverted microscope (TM2000; Nikon) equipped with fluorescence and phase-contrast optics. Parasagittal cerebellar slices were prepared from postnatal days 14 and 21 as described by Vicini et al. (2001). All recordings were performed at room temperature (24–26°C) from neurons maintained for 6–14 DIV. Continuously perfused extracellular solution contained 145 mM NaCl, 5 mM KCl, 1 mM $MgCl_2$, 1 mM $CaCl_2$, 5 mM HEPES, 5 mM glucose, 15 mM sucrose, 0.25 mg/l phenol red, and 10 μM D-serine (all from Sigma), adjusted to pH 7.4 with NaOH. Electrodes were pulled in two stages on a vertical pipette puller from borosilicate glass capillaries (Wiretrol II; Drummond, Broomall, PA) and filled with recording solution containing (in mM): 145 KCl, 10 HEPES, 5 ATP-Mg, 0.2 GTP-Na, and 10 BAPTA, adjusted to pH 7.2 with KOH. Pipette resistance was 5–8 MΩ. Whole-cell voltage-clamp recordings were made at −60 mV with an Axopatch-1D amplifier (Axon Instruments, Union City, CA), and access resistance was monitored throughout the recordings. Capacitance was calculated from a transient current response to a hyperpolarizing 10 mV pulse. Currents were filtered at 1 kHz with an 8-pole low-pass Bessel filter, digitized at 5 kHz using an IBM-compatible microcomputer equipped with Digidata 1322A data acquisition board and pClamp9 software (both from Axon Instruments). Off-line data analysis, curve fitting, and figure preparation were performed with Clampfit 9 software. Solution was exchanged locally with a Y tube (Murase et al., 1989). mIPSCs were isolated by application of 0.5 μM tetrodotoxin (TTX; Alomone Laboratories). NMDA, 3,3-(2-carboxypiperazine-4-yl)-propyl-1-phosphonate (CPP), MK801, and 1(*S*),9(*R*)-(−)-bicuculline methobromide were obtained from Sigma. Infrequent AMPA-mediated miniature EPSCs were easily identified by the very rapid decay (<2 ms) and excluded from the analysis. mIPSC averages were based on at least 50 events in each cell studied. The decay phase of currents was fitted using a simplex algorithm for least squares exponential fitting routines with triple exponential equation of the form $I(t) = I_1 \times \exp(-t/\tau_1) + I_2 \times \exp(-t/\tau_2) + I_3 \times \exp(-t/\tau_3)$, where I_x is a peak amplitude of a decay component and τ_x is the corresponding decay time constant. To allow for easier comparison of decay times between experimental conditions, the three decay time components were combined into a weighted time constant $\tau_w = [I_1/(I_1 + I_2 + I_3)] \times \tau_1 + [I_2/(I_1 + I_2 + I_3)] \times \tau_2 + [I_3/(I_1 + I_2 + I_3)] \times \tau_3$. Single-channel current records from outside-out patches excised from visually identified varicosities were low-pass filtered at 2 kHz (8-pole Bessel filter) and sampled at 20 kHz. Events lists and amplitude estimates were prepared using the Clampfit 9 software. Superimposed openings and openings of <0.3 ms were excluded from the amplitude analysis. Multi-Gaussian fits to amplitude histograms were performed with a simplex least square interactive procedure with Clampfit 9. Single-channel chord conductances were calculated on assuming a reversal potential of 0 mV and a liquid junction potential of −15 mV. All data are expressed as mean ± SEM, unless otherwise indicated; *p* values represent the results of two-tailed Student's *t* tests with Bonferroni corrections.

Results

NMDA alters the morphology of GABAergic interneurons in cerebellar cultures

We studied the morphological differentiation of cerebellar neurons from GAD65–eGFP mice. Imaging of cerebellar slices from these mice (Fig. 1*A*) showed that eGFP expression was limited to cerebellar interneurons in the molecular layer (basket and stellate cells). Higher magnification of the molecular layer in these slices can be found in supplemental Figure 1 (available at www.jneurosci.org as supplemental material). We made primary neuronal cultures from the cerebellum of these mice. In these cultures, the majority of neurons are granule cells and ~3% neurons are GABAergic interneurons (Fig. 1*B*,*C*). In young postmitotic GABAergic interneurons (DIV2), treatment with 10, 30, or 100 μM NMDA induces a pronounced change in the size of axonal boutons (Figs. 1*C*, 2) which begins 18–24 h after treatment and is fully established at 72 h after treatment. In addition to this effect, 100 μM NMDA enhanced survival of granule cells and GABAergic interneurons, suggesting a neurotrophic-like role on both cerebellar phenotypes (Fig. 1*B*). BDNF supports survival/differentiation of cerebellar neurons (Gao et al., 1995; Spatkowski and Schilling, 2003), and BDNF availability in these cells can be increased by NMDA treatment (Marini et al., 1998; Bhave et al., 1999). We explored whether the effects seen with NMDA were caused by BDNF. As seen in Figure 1*B*, the magnitude of the survival-promoting effect of 50 ng/ml BDNF and 100 μM NMDA on granule cells was very similar, but BDNF was more effective than NMDA in increasing the survival of eGFP-labeled GABAergic interneurons. The effects of BDNF and NMDA were diminished by anti-BDNF antibodies (Fig. 1*B*). Qualitative observations of fluorescence images indicate substantial changes in the morphology of GABAergic interneurons with both NMDA and BDNF. However, although BDNF increased the overall complexity of the neuronal arbor, NMDA treatment selectively enhanced the size of the axonal varicosities (Fig. 1*C*).

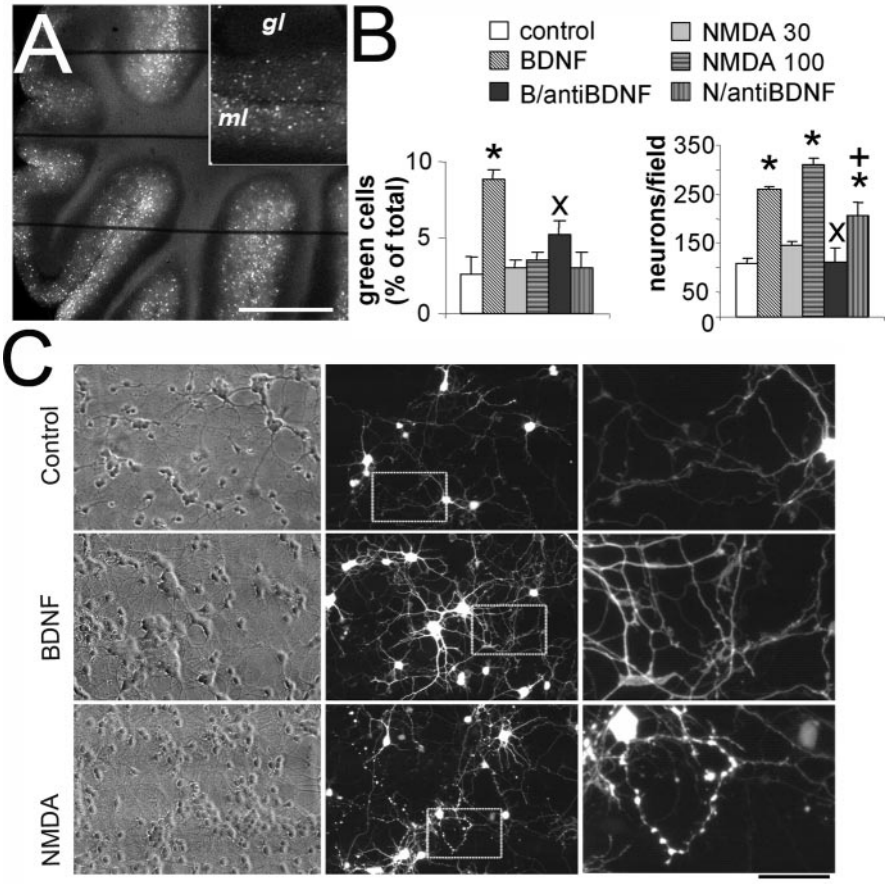

Figure 1. NMDA alters the morphology of GABAergic interneurons in cerebellar cultures. ***A***, A microphotograph of a live cerebellar slice from an adult GAD65– eGFP mouse that illustrates that eGFP-positive neurons are located in the molecular layer (ml) but not in the granule layer (gl). The horizontal lines are the strings of the grid that hold the slice under the microscope. Scale bar: 1 mm; inset, 500 μm. ***B***, Survival of cerebellar neurons (expressed as total number of neurons counted in at least five fields of 400 × 500 μm per coverslip in six coverslips from four distinct cultures) was increased by both NMDA (100 μM) and BDNF (50 ng/ml) treatments. Although NMDA increased the absolute number of green cells because it increased the total number of neurons, the percentage of eGFP-labeled GABAergic interneurons was increased only by BDNF treatment. A lower dose of NMDA (30 μM) failed to affect survival. The effect of treatment with anti-BDNF antibodies (10 μg/ml) is reported for both BDNF (B/anti-BDNF) and NMDA 100 μM (N/anti-BDNF). *$p < 0.01$, significant increase compared with controls; $^{+}p < 0.05$, significant decrease compared with 100 μM NMDA; $^{\times}p < 0.01$, significant decrease compared with BDNF. ***C***, Cerebellar cultures at DIV7 grown for 5 d in the absence (top) or the presence of 50 ng/ml BDNF (middle) or 100 μm NMDA (bottom). Qualitative observations of fluorescence images indicate substantial changes in the morphology of GABAergic interneurons: BDNF increased the complexity of the neuritic tree, whereas NMDA treatment selectively enhanced the size of the axonal varicosities. Scale bar: 90 μm; inset, 26 μm.

The action of BDNF on neuritic tree extension was not investigated quantitatively. We quantified instead the extent of presynaptic bouton enlargement in axons of cerebellar GABAergic interneurons in primary culture (Fig. 2). Analysis of eGFP-labeled varicosities was performed by thresholding the eGFP images at the same intensity value after background subtraction. As shown in Figure 2*A*, eGFP fluorescence in the varicosities well matched GAD65 immunostaining. The density of synaptic boutons was 2.5 ± 0.3 per 10 μm for control cultures, and it was not significantly different in all other experimental conditions tested. NMDA treatment increases the size of the eGFP-positive boutons, and MK801 blocked this action (Fig. 2). The effect of NMDA on bouton size is concentration dependent, and it can be seen at concentration as low as 10 μM NMDA (Fig. 2*B*, left). We also quantified in a smaller subset of experiments the size of the varicosities using GAD65 immunostaining with similar results (data not shown). The effect induced by NMDA was completely blocked by the noncompetitive antagonist of NMDA receptors, MK801 (10 μM) (Fig. 2*B*, right). Endogenous released glutamate is as effective as NMDA because maintaining the cells in depolarizing conditions (25 mM KCl) increased the size of the boutons (Studler et al., 2002) to the same extent as 30 μM NMDA (Fig. 2*B*, left), and this effect is also completely blocked by MK801 (Fig. 2*B*, right). In cells grown in the presence of 10 μM MK801 for 5 d, we failed to observe significant changes in both size and density of varicosities (Fig. 2*B*, right). The action of 100 μM NMDA was not altered by anti-BDNF antibodies (Fig. 2*B*, right). The size of varicosities in axons of interneurons increased with time *in vitro*, because in control cultures at DIV14 it was 379 ± 23% larger (19 axonal segments) than at DIV7. Together, these results suggest

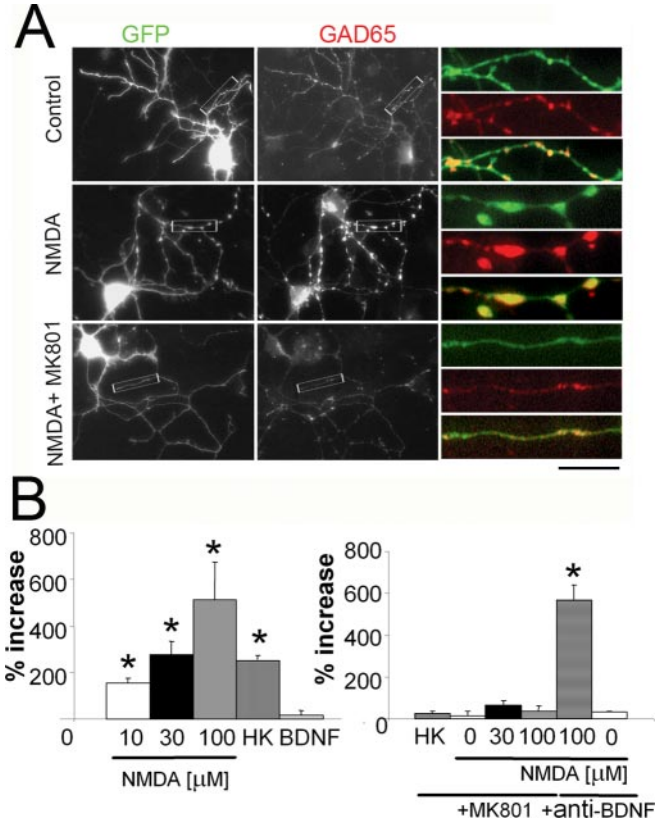

Figure 2. Enlargement of GABAergic boutons induced by NMDA. ***A***, A comparison of eGFP-labeled neurons in control cultures and in cultures treated with 100 μM NMDA (NMDA) or with 100 μM NMDA plus 10 μM MK801 (NMDA + MK801). Colocalization (yellow) of eGFP-filled varicosities (green) and the GABAergic presynaptic marker GAD65 (red). At higher magnification to the right, the eGFP fluorescence distribution (top) is compared with GAD65 immunostaining (middle), and overlapped images illustrate the colocalization (bottom). Note that NMDA treatment increases the size of the eGFP-positive boutons, and MK801 blocked this action. Scale bar: 30 μm; insets, 7 μm. ***B***, Summary results on the analysis of eGFP-labeled varicosities in axons of cerebellar GABAergic interneurons grown in distinct culture conditions. Left, The percentage increase in the area of the varicosities induced by 10, 30, and 100 μM NMDA, 25 mM KCl (HK), and 50 ng/ml BDNF. The area of varicosities in the control group was $0.75 \pm 0.18\ \mu m^2$. Right, The effects of NMDA receptor blockade (10 μm MK801) and blockade of ambient BDNF (10 μg/ml anti-BDNF antibody) on NMDA induced increase in the size of the varicosities. In addition, it is shown that the effect of endogenously released glutamate in high potassium induced varicosity enlargement. Data are derived from at least 30 segments in each experimental group from six separate cultures. *$p < 0.01$, statistical significance compared with controls.

that activation of NMDA receptors on GABAergic interneurons induced enlargement of axonal varicosities. To further investigate the relationship between what was observed for varicosities *in vitro* and the occurrence of these axonal enlargements *in vivo*, we studied confocal stacks of images of molecular layer varicosities taken from cerebellar slices from GAD65–eGFP mice at three distinct developmental ages (P7, P14, and P21). As seen in supplemental Figure 1 (available at www.jneurosci.org as supplemental material), varicosities could be observed in slices from mice at both P14 and P21, but only very faint axons were seen at P7.

To better assess the characteristics of presynaptic varicosities, cerebellar cultures from GAD65–eGFP mice at DIV8 were fixed and immunostained with antibodies against synapsin 1, a prominent presynaptic protein that interacts with actin and the vesicular pool (De Camilli et al., 1990), and VAMP2, an integral protein of the vesicular membrane involved in the exocytotic process (Weber et al., 1998). Figure 3 illustrates examples of axonal segments in which eGFP is compared with immunostaining for synapsin1 or VAMP2 in control and in 100 μM NMDA-treated cultures. Colocalization of eGFP with these presynaptic markers was remarkable. At DIV7 to DIV8, 85 ± 4% of eGFP-positive boutons were colocalized with synapsin 1, and 74 ± 10% with VAMP2. These values were not significantly affected by NMDA treatment (Fig. 3*A*, % Positive). The comparison between average intensity of fluorescent staining (Fig. 3*A*, Average Intensity) was not significantly different in treated and control cultures. On the contrary, the integrated fluorescence intensity, which takes into account the area of the varicosity, significantly increased with NMDA treatment for both synapsin1 and VAMP2 staining (Fig. 3*A*, Integrated Intensity). This suggested that the enlargement of the varicosities corresponded to an increase in the size of presynaptic GABAergic terminals. In addition, we measured the accumulation of the styril dye FM4-64 to estimate functional release sites (Fernandez-Alfonso and Ryan, 2004). As seen in Figure 3*A*, enlarged varicosities accumulate more dye than untreated samples. In axonal segments from cultures at DIV7 to DIV8, 65 ± 11% of eGFP-positive boutons were colocalized with FM4-64. With NMDA treatment, eGFP–FM4-64 colocalization and average fluorescence intensity slightly increased, but the integrated fluorescence intensity was significantly larger (Fig. 3*A*). As a control, we investigated the effect of NMDA treatment on the expression of vesicular glutamate transporters (vGlut-1 and vGlut-2), presynaptic markers specific for excitatory synapses that are expressed in developing cerebellar granule cells (Wojcik et al., 2004). As seen in Figure 3*B*, NMDA treatment failed to increase area, intensity, or density of vGlut-1 and vGlut-2 boutons. Overall, these findings reveal that NMDA treatment selectively enlarges GABAergic presynaptic terminals, along with an increase in their vesicular pool. Next, we sought to establish whether these anatomical changes were functionally relevant.

NMDA increased spontaneous synaptic release from GABAergic interneurons in cerebellar cultures

Spontaneous synaptic release from GABAergic terminals was investigated with whole-cell recordings of mIPSCs from cerebellar granule neurons (Ortinski et al., 2004). Granule cells were voltage-clamped at −60 mV, and with symmetrical Cl^- solution, mIPSCs were observed as inward currents (Fig. 4*A*). mIPSCs were recorded from 17 cells in four distinct sets of control cultures at DIV7 to DIV8. As shown in Purkinje neurons (Glitsch and Marty, 1999; Duguid and Smart, 2004) and interneurons (Glitsch and Marty, 1999) in cerebellar slices, application of NMDA (20 μM) induced a sudden and persistent increase in the mIPSC frequency (Fig. 4*A*,*C*) with no change in amplitude or decay kinetics (Fig. 4*B*,*C*). Although NMDA was applied in the presence of 1 mM Mg^{2+}, a small persistent inward current was observed together with the mIPSCs. We then studied mIPSCs in 18 cells from three distinct cultures that were chronically treated with NMDA. In DIV7 cultures pre-exposed to 30 μM NMDA for 5 d, there was an approximately threefold increase in mIPSC frequency over control cells. There were no kinetic changes seen in these mIPSCs (Fig. 5), and amplitude was unchanged (42 ± 4 vs 46 ± 5 pA). In these cells, acute NMDA application could still increase mIPSC frequency, although to a much smaller extent (Fig. 5*C*). In five granule neurons in control cultures at DIV8, the increased mIPSC frequency induced by application of 20 μM NMDA remained unchanged for at least 30 min (supplemental Fig. 2, available at www.jneurosci.org as supplemental material). NMDA-induced mIPSC frequency increase was unchanged in one of these neurons in which recording was maintained for 1 hr.

When mIPSCs were recorded from granule cells grown in

culture for 2 weeks ($n = 15$), mIPSC frequency increased, and decay time became faster (Fig. 5*C*) (Ortinski et al., 2004). In these cells, NMDA (20 μM) application failed to increase mIPSC frequency (Fig. 5*C*). NMDA was also ineffective in increasing mIPSC frequency in cells treated with NMDA for 12 d ($n = 14$; DIV14) (Fig. 5*C*). As a consequence of chronic NMDA treatment, however, mIPSC frequency in granule cells at DIV14 increased 2.5-fold compared with controls (Fig. 5*C*). In parallel experiments, cells were treated with BDNF and MK801 plus NMDA; here, mIPSC frequency was similar to control values (0.43 ± 0.12 and 0.27 ± 0.05 Hz).

We also recorded mIPSCs from eGFP-positive neurons located in the molecular layer of cerebellar slices from GAD65–eGFP mice. mIPSC frequency increased from P14 to P21, and perfusion with 20 μM NMDA significantly increased mIPSC frequency in cells from mice at P14 but not at P21 (Fig. 5*C*).

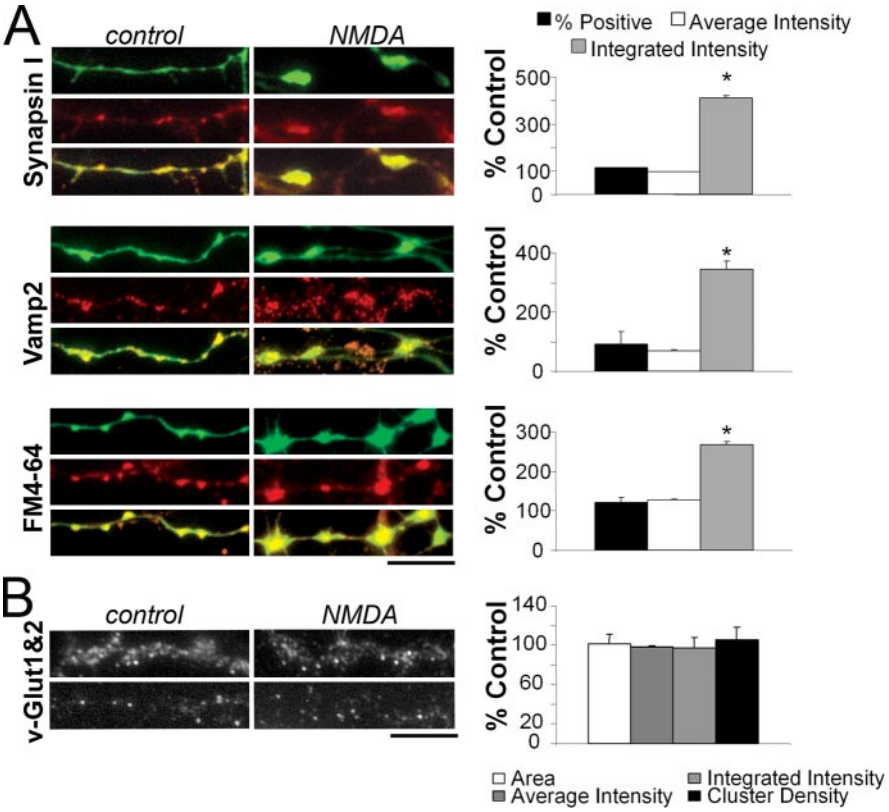

Figure 3. Enlarged GABAergic varicosities are active release units that express synaptic markers. ***A***, Enlarged GABAergic terminals express synapsin1 and VAMP2 and accumulate the styril dye FM4-64. Left, Representative images of cultures from GAD65–eGFP mice at DIV8 grown in the absence (control) or the presence of 100 μm NMDA (NMDA). Samples were fixed and immunostained with antibodies against synapsin1 or VAMP2 or loaded with the styril dye FM4-64. eGFP (green), synapsin1, VAMP2, or FM4-64 (red) and the colocalization is shown in overlapped insets at the bottom. Right, Summary data on the analyses of colocalized eGFP with synapsin, VAMP2, and FM4-64 showing the percentage of positive GABAergic terminals for the different probes and the averaged and integrated fluorescence intensity for each probe in a given varicosity. Data are derived from at least 21 segments in each experimental group from three separate cultures. *$p < 0.01$, statistical significance compared with controls. ***B***, Lack of effect of NMDA on the size of glutamatergic terminals. Left, vGlut-1 and vGlut-2 immunostaining in cultured cerebellar neurons grown for 8 d in control conditions or treated with 100 μM NMDA. Right, Summary results of the effect of NMDA on glutamatergic terminals. The area of each cluster, cluster density, and averaged and integrated intensity are expressed as percentage of untreated samples. Data derive from 13 segments from two separate cultures. Scale bars: ***A, B***, 8 μm.

NMDA currents from presynaptic terminals

Being able to unambiguously identify the interneurons with the eGFP labeling permitted direct recording of their enlarged presynaptic boutons and allowed us to test the hypothesis that NMDA receptor channels were present and functionally active. As shown in Figure 6*A*, axonal varicosities could be easily observed from overlapped DIC and fluorescence microphotographs, being often in close proximity to postsynaptic granule cells. While recording from such a terminal, application of Mg^{2+}-free solution elicited repetitive action currents of small size (Fig. 6*B*), suggesting a propagation of unclamped action potential from the generating region of the axon. Direct application of NMDA 20 μM together with TTX in a Mg^{2+}-free solution generated inward currents in the varicosity that was abolished by the NMDA receptor antagonist CPP (10 μM). On average, such currents in the terminals were 15 ± 3 pA ($n = 9$) when terminals were at least 50 μm from the interneuron somata. In three terminals in close proximity to the cell body, NMDA elicited a large current (>100 pA), and the occurrence of mIPSCs was detected. These currents are likely generated in the cell body of the GABAergic interneuron and propagated to the varicosity. To directly determine the properties of NMDA receptor channels in the varicosities, we excised outside-out patches. Nine of 23 (39%) patches did not have measurable currents. In the 14 remaining patches, NMDA-induced current was 9 ± 4 pA; these currents were abolished by 10 μM CPP (Fig. 6*C*). As illustrated in Figure 6*C* (bottom), the histogram of amplitude distribution showed the occurrence of openings at four distinct conductance levels. Conductance levels were 50.1 ± 1.1 and 41.2 ± 1.3 pS and 35.1 ± 0.7 and 19.3 ± 1.1 pS ($n = 10$). In additional experiments ($n = 6$), we recorded from granule cells that were contacted by a varicosity as in the example in Figure 6*A*. After mechanical stimulation of the varicosity with a second patch pipette, a large discharge of mIPSCs was recorded as in the example shown in Figure 6*D*. After recovery of basal mIPSC frequency, perfusion with bicuculline methobromide abolished all currents ($n = 5$). No evoked response was seen in the presence of the $GABA_A$ receptor antagonist. These results provide the first direct measurements of NMDA responses in an inhibitory presynaptic neuron.

Discussion

One of the best examples of presynaptic regulation by excitatory amino acids is the action of glutamate receptor agonists on mIPSC frequency in developing basket/stellate cells in cerebellar slices (Bureau and Mulle, 1998; Glitsch and Marty, 1999; Duguid and Smart, 2004; Huang and Bordey, 2004). Our data extend these results to cerebellar neurons in culture and show that with NMDA treatment the size of the GABAergic boutons along the axons of developing GABAergic neurons in culture increased in parallel with spontaneous transmitter release.

Trophic effects of BDNF and NMDA on cerebellar basket/stellate interneurons

A possibility to explain the NMDA action is that it occurs via a neurotrophic factor. BDNF increases dendritic branching and

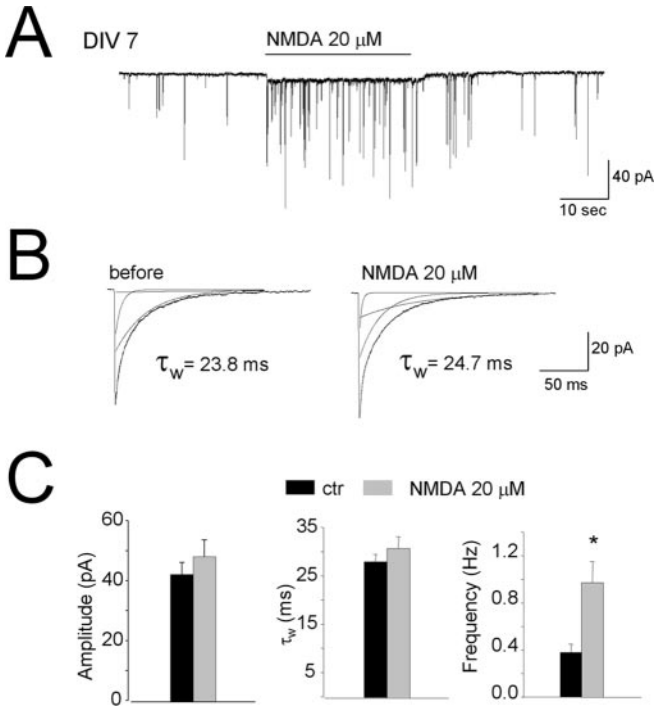

Figure 4. NMDA increase the amplitude and frequency of mIPSCs. Effect of acute application of NMDA on GABAergic mIPSCs recorded from control cerebellar granule cells at DIV7 to DIV8. ***A***, Representative current record from a granule cell at DIV7. Horizontal bar corresponds to the application of NMDA (20 μM). ***B***, Averaged mIPSCs recorded before (left) and during NMDA exposure (right). Currents were fitted by using a triple-exponential function yielding weighted time constants (τ_w) calculated as described in Materials and Methods. ***C***, Summary of the effect of acute NMDA exposure on mIPSC amplitude, τ_w, and frequency.

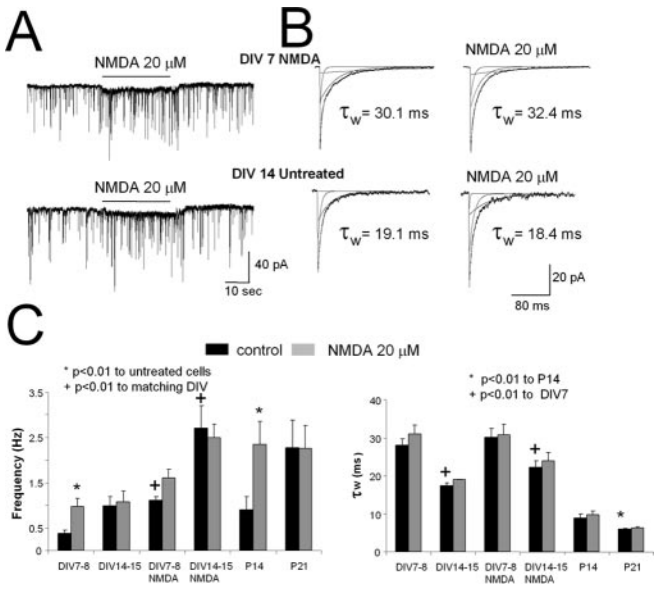

Figure 5. Increase in mIPSCs by NMDA is prevented by development and NMDA chronic treatment. ***A***, A comparison of mIPSC records from cerebellar granule cells at DIV7 cultured in the presence of NMDA (20 μM, top, DIV7 NMDA) and cells at DIV14 grown in control conditions (bottom, DIV14 Untreated). Horizontal bar corresponds to the acute application of NMDA (20 μM). ***B***, Averaged mIPSCs recorded before (left) and during acute NMDA application (right) from cells at DIV7 cultured in the presence of NMDA (20 μm, top) and cells at DIV14 in control conditions (bottom). ***C***, Summary of the effect of the chronic and acute NMDA exposure on GABAergic mIPSC frequency and τ_w values in cultures at DIV7 to DIV8 and DIV14 to DIV15. For comparison are also shown mIPSC frequency and NMDA action in eGFP-positive molecular layer interneurons in slices from GAD65– eGFP mice at P14 and P21.

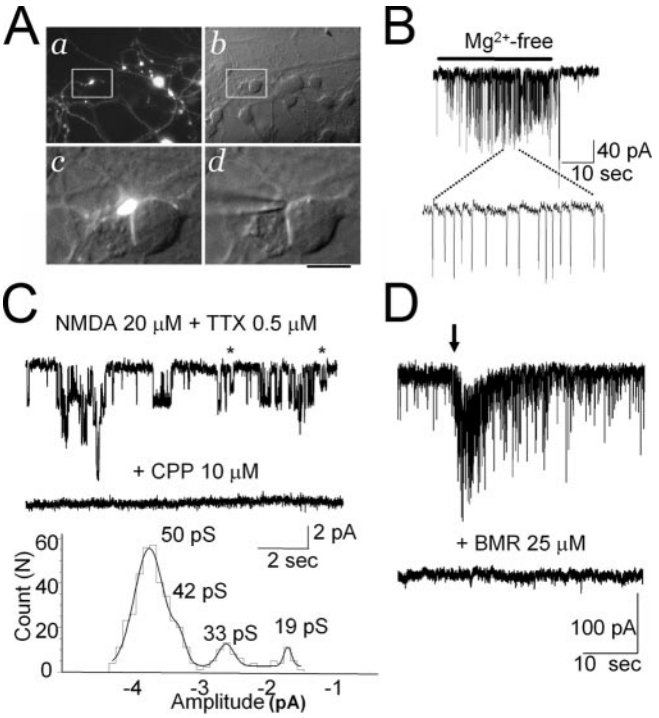

Figure 6. Recordings from presynaptic terminals. ***A***, Microphotograph of cerebellar neurons at DIV8 in an NMDA-treated culture. ***a*** shows eGFP-positive neurons and axons with large varicosities. The same field is shown to the right with DIC Nomarski optics (***b***). White box inserts are magnified below showing a varicosity (eGFP/DIC-Nomarski; ***c***) in close proximity to the cell body of a granule cell. The tip of a patch pipette touching the varicosity is shown in ***d***. Scale bars: ***a***, ***b***, 30 μm; ***c***, ***d***, 7 μm. ***B***, Whole-cell recording from an eGFP-labeled varicosity illustrating repetitive action currents consequent to the increase excitability of the GABAergic interneuron after removal of Mg^{2+} from the bath solution. ***C***, NMDA-elicited channel currents in an outside-out patch excised from eGFP-labeled varicosity are abolished by the NMDA receptor antagonist CPP. Openings at a lower conductance levels are indicated with asterisks. For illustration, records were filtered at 0.9 kHz. The bottom panel illustrates the single-channel current amplitude distribution in this patch with an indication of the conductance levels derived from fitting of the distribution with the sum of four Gaussian curves. ***D***, Whole-cell recording from a granule cell illustrating a strong increase in the frequency of occurrence of mIPSCs when a patch pipette mechanically stimulated a proximal eGFP-labeled varicosity as that illustrated in ***A***, ***c***. The bottom trace illustrates recording in the presence of bicuculline methobromide (BMR) 25 μM.

promotes axonal growth in cerebellar Purkinje and granule cells (Gao et al., 1995; Hirai and Launey, 2000) as well as cerebellar interneurons (Spatkowski and Schilling, 2003). Cerebellar granule cells synthesize BDNF, and its release is regulated by NMDA receptors (Marini et al., 1998). Indeed, we observed that both NMDA and BDNF increase survival of all cerebellar cells and granule cells, as reported previously (Balázs et al., 1989; Burgoyne et al., 1993; Gao et al., 1995), and survival of eGFP-labeled interneurons. Part of the NMDA effect is attributable to BDNF, as the treatment with anti-BDNF antibodies suggests and as shown previously (Marini et al., 1998; Bhave et al., 1999). We also report a selective BDNF effect on the survival of basket/stellate cells. However, the morphogenic action of BDNF was very different from that of NMDA because the former failed to increase the size of the synaptic boutons over control values. These data argue against NMDA action on the varicosities through an increased availability of BDNF, as also shown by the lack of blockade of the NMDA effect with anti-BDNF antibodies.

Axonal varicosities are GABAergic synapses

Several independent findings identified axonal varicosities as GABAergic synapses. First, they express GAD65, a GABA-

synthesizing enzyme subtype associated with synaptic vesicles (Jin et al., 2003). Second, they express the presynaptic vesicle associated proteins synapsin 1 and VAMP2. The increase in VAMP2 staining of presynaptic varicosities with NMDA treatment suggests an increase in the size of the vesicular pool (Krueger et al., 2003). Third, a large number of varicosities can be loaded with the styril dye FM4-64, a marker of functional release sites (Fernandez-Alfonso and Ryan, 2004). Fourth, varicosities are facing clusters of postsynaptic $GABA_A$ receptors (Ortinski et al., 2004), and they can generate burst discharge of mIPSCs after mechanical stimulation with a patch pipette.

The presence of enlarged varicosities in the axons of interneurons in cerebellar molecular layer has been well established (Palay and Chan-Palay, 1974), and patch-clamp recordings from these varicosities in slices revealed several different subtypes of potassium channels (Southan and Robertson, 1998). Morphological changes in basket cell terminals with development have been reported previously (Pouzat and Hestrin, 1997), suggesting enlargement of varicosities. We observed similar changes with development in the size of these varicosities *in vivo* and *in vitro*.

Functional consequence of NMDA action at inhibitory synapses

The increased size of presynaptic varicosities with age *in vitro* or with NMDA treatment is accompanied by a pronounced increase in the frequency of mIPSCs, but not in their amplitude. This suggests that the number of vesicles spontaneously released increases, but the response to a single vesicle does not change. Increases in mIPSCs frequency with development have been reported in recordings from interneurons in cerebellar slices along with the loss of the acute action of excitatory amino acids (Bureau and Mulle, 1998; our results). We show that with both NMDA treatment and development in culture, the acute NMDA-induced action on mIPSCs occurrence is lost. Together, these results suggest that as culture develops, glutamate release from granule neurons is sufficient to slowly induce the increase in mIPSC frequency and that the NMDA treatment can both mimic and accelerate this effect.

Our result may be related to *in vivo* findings of developmental changes in inhibitory synaptic efficacy in cerebellar neurons. Frequency of occurrence of spontaneous and miniature IPSC increase with development in stellate neurons (Bureau and Mulle, 1998; our results). NMDA increases mIPSC frequency in Purkinje and stellate neurons in cerebellar slices, but reduces the amplitude of evoked IPSCs (Glitsch and Marty, 1999). Thus, the net action of the activation of presynaptic NMDA receptor is to decrease rather than enhance evoked synaptic transmission between basket/stellate cells and their targets. Indeed, strong reduction of the efficacy of coupling between individual cerebellar interneuron and Purkinje cells has been reported in the developing cerebellum (Pouzat and Hestrin, 1997). As proposed by Bureau and Mulle (1998), the increase in mIPSC occurrence is likely related to an increase in the release sites together with a decrease in release probability at each site. Large GABAergic terminals may provide the anatomical substrate for the increase number of release sites, with decreased release probability. This hypothesis is also supported by the lack of changes in the density of presynaptic boutons with NMDA treatment in our culture. Interestingly, as shown for Purkinje to cerebellar nuclear synapses (Telgkamp et al., 2004) large multisite presynaptic terminals may have an important physiological role in the maintenance of high-frequency inhibitory synaptic transmission.

The location of presynaptic NMDA receptors

Duguid and Smart (2004) have recently given an important contribution to the understanding of presynaptic regulation of GABAergic neurotransmission in the cerebellum. They reported that the NMDA action on presynaptic GABAergic terminal is part of a physiological regulation termed depolarization-induced potentiation of inhibition. This effect is attributable to presynaptic NMDA receptors located on axons if not directly on the presynaptic terminals (Petralia et al., 1994; Glitsch and Marty, 1999; Duguid and Smart, 2004; Huang and Bordey, 2004). Additional arguments in favor of this hypothesis is the lack of synaptic NMDA receptor activation in cerebellar interneurons and the mismatch between the size of NMDA currents generated in cell body and the mIPSCs frequency increase (Glitsch and Marty, 1999). However, Clark and Cull-Candy (2002), while supporting the lack of synaptic NMDA receptors in GABAergic interneurons in the molecular layer, demonstrated with direct iontophoretic glutamate applications that these neurons are unique because NMDA responses are strong when generated in extrasynaptic somatodendritic locations but not in axons. Although expression of distinct NMDA receptor subunits has been shown with immunostaining in all anatomical compartments of molecular layer interneurons in culture (Duguid and Smart, 2004), this result does not exclude the possibility of a lower density of NMDA receptors in axon that may underlie the findings of Clark and Cull-Candy (2002). To address the localization of axonal NMDA receptors, we directly measured electrophysiological responses triggered by NMDA in the enlarged GABAergic boutons. The results of our study indicate that although NMDA currents could be recorded from presynaptic terminals, the electrotonic current propagation along the axon can be quite considerable. Unclamped action potential and inhibitory synaptic currents can be recorded from the terminals, and the magnitude of these currents is greater if the terminal is close to the cell body. Thus, somatodendritic NMDA receptor activation can be transmitted to the terminals despite the presence of TTX. Therefore NMDA receptors on the cell body and dendritic tree are likely to contribute to the current recorded in the terminal and the enhancement of mIPSC frequency. However, our data directly demonstrate the presence of NMDA receptors in axonal boutons because NMDA channel currents were recorded in more than half of the outside-out membrane patches excised from varicosities. Interestingly, several different conductance levels were observed for NMDA channels in these terminals, suggesting the expression of receptor subtypes with NR2C and/or NR2D subunit with decreased Mg^{2+} sensitivity (Cull-Candy et al., 2001). These data are consistent with the reported low sensitivity to Mg^{2+} blockade of acute NMDA action on mIPSC frequency in slices (Glitsch and Marty, 1999).

Our results suggest that NMDA receptors are located in the axon, dendrite, and cell body of cerebellar interneurons in culture, and these all influence mIPSC release. A global decrease in functional NMDA receptors in GABAergic interneurons as a consequence of desensitization and downregulation after NMDA treatment could explain the loss of acute NMDA effects on mIPSCs. However, the action of NMDA on mIPSC frequency did not desensitize, at least in the short term allowed by the electrophysiological recording. Furthermore, active NMDA channels were seen in varicosities of NMDA-treated cells. It is appealing to speculate that the disappearance of the acute effect of NMDA with NMDA treatment and development is not caused by the loss of NMDA receptors, but rather to a permanent alteration of the release machinery in the bouton, perhaps linked to long-term

changes in intracellular calcium concentration. This is further supported by the results of Duguid and Smart (2004) on the developmental loss of the inhibitory synaptic plasticity in Purkinje neurons.

Conclusions

Open questions from our data are whether the regulation of inhibitory transmission is a developmental trend or it is compensatory to the enhanced excitability induced by excitatory amino acids. If the latter were true, one could envision our results as a homeostatic regulation between excitation and inhibition, in which increased mIPSC frequency can act as a tonic brake for excitability. A decrease in unitary, action potential-evoked inhibitory synaptic efficacy may also be a necessary consequence to excitation. However, it is more likely instead that the action of NMDA has simply a trophic role in the consolidation of inhibition. Further studies will address these issues.

In summary, we provided morphological correlates to the finding of a presynaptic action of NMDA in cerebellar basket/stellate interneurons, insights on possible mechanisms of NMDA action on mIPSC frequency, and we established a model *in vitro* that should allow a better understanding of the interplay between excitation and inhibition.

References

Balázs R, Hack N, Jorgensen OS, Cotman CW (1989) *N*-methyl-D-aspartate promotes the survival of cerebellar granule cells: pharmacological characterization. Neurosci Lett 101:241–246.

Bhave SV, Ghoda L, Hoffman PL (1999) Brain-derived neurotrophic factor mediates the anti-apoptotic effect of NMDA in cerebellar granule neurons: signal transduction cascades and site of ethanol action. J Neurosci 19:3277–3286.

Borodinsky LN, Coso OA, Fiszman ML (2002) Contribution of Ca^{2+} calmodulin-dependent protein kinase II and mitogen-activated protein kinase kinase to neural activity-induced neurite outgrowth and survival of cerebellar granule cells. J Neurochem 80:1062–1070.

Brager DH, Luther PW, Erdelyi F, Szabo G, Alger BE (2003) Regulation of exocytosis from single visualized GABAergic boutons in hippocampal slices. J Neurosci 23:10475–10486.

Bureau I, Mulle C (1998) Potentiation of GABAergic synaptic transmission by AMPA receptors in mouse cerebellar stellate cells: changes during development. J Physiol (Lond) 509:817–831.

Burgoyne RD, Graham ME, Cambray-Deakin M (1993) Neurotrophic effects of NMDA receptor activation on developing cerebellar granule cells. J Neurocytol 22:689–695.

Chang S, De Camilli P (2001) Glutamate regulates actin-based motility in axonal filopodia. Nat Neurosci 4:787–793.

Clark BA, Cull-Candy SG (2002) Activity-dependent recruitment of extrasynaptic NMDA receptor activation at an AMPA receptor-only synapse. J Neurosci 22:4428–4436.

Cull-Candy S, Brickley S, Farrant M (2001) NMDA receptor subunits: diversity, development and disease. Curr Opin Neurobiol 11:327–335.

De Camilli P, Benfenatti F, Valtorta F, Greengard P (1990) The synapsins. Annu Rev Cell Biol 6:443–450.

Duguid IC, Smart TG (2004) Retrograde activation of presynaptic NMDA receptors enhances GABA release at cerebellar interneuron-Purkinje cell synapses. Nat Neurosci 7:525–533.

Eccles JC, Ito M, Szentágothai J (1967) The cerebellum as a neuronal machine. New York: Springer.

Fernandez-Alfonso T, Ryan TA (2004) The kinetics of synaptic vesicle pool depletion at CNS synaptic terminals. Neuron 41:943–953.

Galarreta M, Erdélyi F, Szabó G, Hestrin S (2004) Electrical coupling among irregular-spiking GABAergic interneurons expressing cannabinoid receptors. J Neurosci 24:9770–9778.

Gallo V, Kingsbury A, Balázs R, Jorgensen OS (1987) The role of depolarization in the survival and differentiation of cerebellar granule cells in culture. J Neurosci 7:2203–2213.

Gao WQ, Zheng JL, Karihaloo M (1995) Neurotrophin-4/5 (NT-4/5) and brain-derived neurotrophic factor (BDNF) act at later stages of cerebellar granule cell differentiation. J Neurosci 15:2656–2667.

Glitsch M, Marty A (1999) Presynaptic effects of NMDA in cerebellar Purkinje cells and interneurons. J Neurosci 19:511–519.

Hirai H, Launey T (2000) The regulatory connection between the activity of granule cell NMDA receptors and dendritic differentiation of cerebellar Purkinje cells. J Neurosci 20:5217–5224.

Huang H, Bordey A (2004) Glial glutamate transporters limit spillover activation of presynaptic NMDA receptors and influence synaptic inhibition of Purkinje neurons. J Neurosci 24:5659–5669.

Jin H, Wu H, Osterhaus G, Wei J, Davis K, Sha D, Floor E, Hsu CC, Kopke RD, Wu JY (2003) Demonstration of functional coupling between gamma-aminobutyric acid (GABA) synthesis and vesicular GABA transport into synaptic vesicles. Proc Natl Acad Sci USA 100:4293–4298.

Krueger SR, Kolar A, Fitzsimonds M (2003) The presynaptic release apparatus is functional in the absence of dendritic contact and highly mobile within isolated axons. Neuron 40:945–957.

Lopez-Benedito G, Sugress K, Erdélyi F, Szabó G, Molnár Z, Poulsen O (2004) Preferential origin and layer destination of GAD65–eGFP cortical interneurons. Cereb Cortex 14:1122–1133.

Ma L, Zablow L, Kandel ER, Siegelbaum SA (1999) Cyclic AMP induces functional presynaptic boutons in hippocampal CA3-CA1 neuronal cultures. Nat Neurosci 2:24–30.

Marini AM, Rabin SJ, Lipsky RH, Mocchetti I (1998) Activity-dependent release of brain-derived neurotrophic factor underlies the neuroprotective effect of *N*-methyl-D-aspartate. J Biol Chem 273:29394–29399.

Mellor JR, Merlo D, Jones A, Wisden W, Randall AD (1998) Mouse cerebellar granule cell differentiation: electrical activity regulates the $GABA_A$ receptor $\alpha 6$ subunit gene. J Neurosci 18:2822–2833.

Murase K, Ryu PD, Randic M (1989) Excitatory and inhibitory amino acids and peptide-induced responses in acutely isolated rat spinal dorsal horn neurons. Neurosci Lett 103:56–63.

Ortinski PI, Lu C, Takagaki K, Fu Z, Vicini S (2004) Expression of distinct α subunits of $GABA_A$ receptor regulates inhibitory synaptic strength. J Neurophysiol 92:1718–1727.

Palay SL, Chan-Palay V (1974) Cerebellar cortex: cytology and organization New York: Springer.

Petralia RS, Wang YX, Wenthold RJ (1994) The NMDA receptor subunits NR2A and NR2B show histological and ultrastructural localization patterns similar to those of NR1. J Neurosci 14:6102–6120.

Pouzat C, Hestrin S (1997) Developmental regulation of basket/stellate cell–Purkinje cell synapses in the cerebellum. J Neurosci 17:9104–9112.

Resink A, Villa M, Benke D, Hidaka H, Mohler H, Balázs R (1996) Characterization of agonist-induced down-regulation of NMDA receptors in cerebellar granule cell cultures. J Neurochem 66:369–377.

Southan AP, Robertson BJ (1998) Patch-clamp recordings from cerebellar basket cell bodies and their presynaptic terminals reveal an asymmetric distribution of voltage-gated potassium channels. J Neurosci 18:948–955.

Spatkowski G, Schilling K (2003) Postnatal dendritic morphogenesis of cerebellar basket and stellate cells in vitro. J Neurosci Res 72:317–326.

Studler B, Fritschy JM, Brunig I (2002) GABAergic and glutamatergic terminals differentially influence the organization of GABAergic synapses in rat cerebellar granule cells in vitro. Neuroscience 114:123–133.

Tashiro A, Dunaevsky A, Blazeski R, Mason CA, Yuste R (2003) Bidirectional regulation of hippocampal mossy fiber filopodial motility by kainate receptors: a two-step model of synaptogenesis. Neuron 38:773–784.

Telgkamp P, Padgett DE, Ledoux VA, Woolley CS, Raman IM (2004) Maintenance of high-frequency transmission at Purkinje to cerebellar nuclear synapses by spillover from boutons with multiple release sites. Neuron 41:113–126.

Ueno S, Zempel JM, Steinbach JH (1996) Differences in the expression of GABA(A) receptors between functionally innervated and non-innervated granule neurons in neonatal rat cerebellar cultures. Brain Res 714:49–56.

Vicini S, Ferguson C, Prybylowski K, Kralic J, Morrow L, Homanics GE (2001) $GABA_A$ receptor $\alpha 1$ subunit deletion prevents developmental changes of inhibitory synaptic currents in cerebellar neurons. J Neurosci 21:3009–3016.

Virginio C, Martina M, Cherubini E (1995) Spontaneous GABA-mediated synaptic currents in cerebellar granule cells in culture. NeuroReport 6:1285–1289.

Weber T, Zemelman BV, McNew JA, Westermann B, Gmachl M, Parlati F, Sollner TH, Rothman JE (1998) SNAREpins: minimal machinery for membrane fusion. Cell 92:759–772.

Wojcik SM, Rhee JS, Herzog E, Sigler A, Jahn R, Takamori S, Brose N, Rosenmund C (2004) An essential role for vesicular glutamate transporter 1 (VGLUT1) in postnatal development and control of quantal size. Proc Natl Acad Sci USA 101:7158–7163.